31st Congress of the International Council of the Aeronautical Sciences

Belo Horizonte, Brazil; September 09-14, 2018

APPLICATION OF HIGH-ROBUSTNESS BEMT FOR SIMULATION OF UAV-VTOL PROPELLER AT LOW/HIGH ADVANCE RATIO

FAN Zhongyun*,, ZHOU Zhou*,**, ZHU Xiaoping****

*** School of Aeronautics, Northwestern Polytechnical University, Xi'an 710072, China**

**** Science and Technology on UAV Laboratory, Northwestern Polytechnical University, Xi'an 710065, China**

Keywords: *Propellers; Blade Element; Neural Networks; VTOL/STOL aircraft; Rotors*

Abstract

For UAV-VTOL propeller design, lots of nonlinear effect should be considered such as low-Re, transonic and large AOA effect. On the other hand, when considering the propeller-wing interaction in the design, the flow details of the propeller, such as circulation, should be obtained. The basic Blade Element Momentum Theory (BEMT) has difficulty analyzing propellers at Low/High advance ratio. In this paper, an improved BEMT is presented for nonlinear wide-range propeller analysis. First, the artificial Neural Networks are used to establish the airfoil performance evaluating model. Second, the BEMT was refined by circulation iteration and is able to analyze propeller at both low/high advance ratio robustly. Third, the analysis examples are presented to shown the accuracy and robustness of the refined BEMT. At last, the inversed BEMT for propeller design is present.

1 Introduction

For the fixed pitch UAV-VTOL propeller, the design process is expected to make reasonable compromises between hovering condition and high speed condition. Currently, the prohibitive computational cost of computational fluid dynamics (CFD) method makes it impossible to conduct a design process directly. Instead, blade element momentum theory (BEMT) is widely used in propeller design for its efficiency in terms of computational time.

Although many scholars have done research on the nonlinear model of airfoil[9]-[11], for UAV-VTOL propeller, there are lots of non-linear effect should be taken into consideration for sectional airfoil analysis, such as low-Re, transonic and large AOA effect. Thus, the sectional airfoil analysis becomes a problem which should be able to conduct multi-nonlinear wide-range analysis. However, the accuracy of BEMT is highly depends on the sectional airfoil information. Therefore, to consider the multi-nonlinear effect, an artificial neural network (ANN) is used at present paper to "learn" and predict the sectional airfoil nonlinear aerodynamic analysis, instead of using CFD directly for airfoil analysis.

On the other hand, when considering the propeller-wing interaction in the design, the flow details of the propeller should be obtained, including the circulation of the blade and induced velocity behind the propeller. BEMT is available for computing the circulation and induced velocity, but when the extreme condition is taken into consideration, BEMT is proved to have bad performance for computing flow details, especially when the stall effect is reached or lift coefficient (C_L) is nearly zero at high J. However，the most scholars studying on BEMT focused on the normal working condition[12]-[15], while the study on extreme condition is insufficient. Therefore, this paper carried out an improvement for BEMT to refine the induced velocity and blade circulation results combined with vortex theory, which helps improving the robustness of BEMT.

At the section 2, an airfoil quick nonlinear analysis model is established using ANN, which is used to predict aero-performance of blade element. Then, the traditional BEMT using ANN and its limitation is discussed at present paper, and the improvement method is carried out at the section 3. As application of this method, a refined BEMT (rBEMT) procedure is developed for propeller wide-range analysis, considering multi-nonlinear effect with high-robustness. At the section 4, rBEMT is proved by numerical examples that it can offer accurate thrust and power prediction at both extremely low/high advance ratio. At last, an inverse BEMT design method is presented.

2 Airfoil Aerodynamic Analysis Model

2.1 BP Neural Network Model

In order to take account of the multi-nonlinear aerodynamic characteristics of blade elements, this paper established a Back Propagation (BP) ANN and discussed its performance. The basic principles of neural networks have been discussed in reference [1]. The author chose a four layers ANN, which contains an input-layer, two hidden-layers and an output-layer. The inputs of the network are Reynolds-number (*Re*), Mach-number (*Ma*) and angle of attack (α), while the outputs are lift, drag and moment coefficients (C_L, C_D, C_M). A double tangent Sigmoid function is used as the transmission function of the hidden layer, while the output layer is linear. In this paper, the moment coefficient is not used, but it is still set as an output for future research on the variable-pitch propeller.

As preliminary study, Clark-Y is used as sample airfoil. Number of samples is 1463. The range and step of the samples are shown as follows. The step of *Re* is small in low Re and large in high *Re*.

Table 1 Range of samples

Input	Start-value	End-value	Step
Re	0.6×10^5	40×10^5	Variable
Ma	0.05	0.55	0.05
α	-3°	15°	3°

Train the BP ANN with those samples and the ANN nonlinear airfoil prediction model will be established.

2.2 Performance of Airfoil Prediction Model

2.2.1 Aerodynamic Characteristics Prediction

Cross-validation shows that most of the prediction relative error will lower than 10%. But when the prediction-value near 0 or α is larger than 10*deg* (strong nonlinear effect), relative error of a few points will larger than 10%. As an example, the prediction of ANN and CFD results are shown in Fig 1~Fig 3, in which $Re=3.0\times10^5$, $Ma=0.4$.

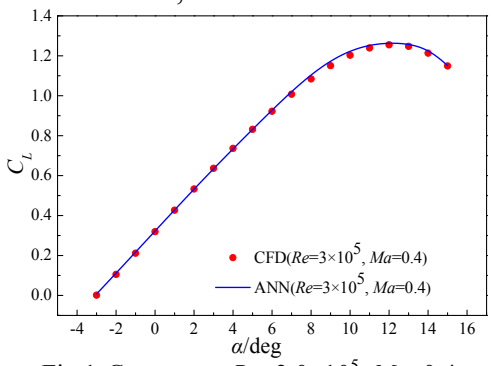

Fig 1 C_L-curve at $Re=3.0\times10^5$, $Ma=0.4$

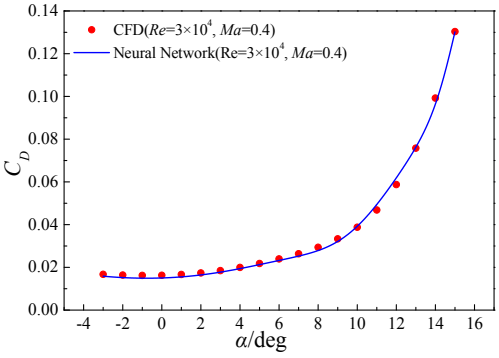

Fig 2 C_D- curve at $Re=3.0\times10^5$, $Ma=0.4$

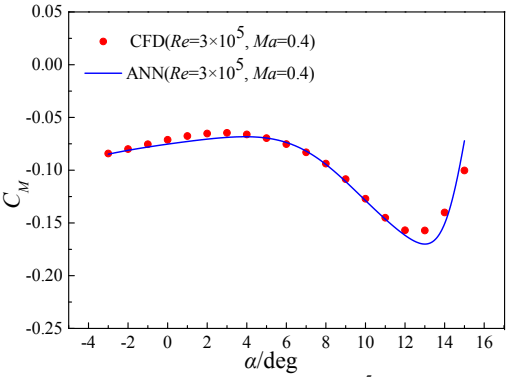

Fig 3 C_M- curve at $Re=3.0\times10^5$, $Ma=0.4$

However, the curves show good consistency between ANN prediction and CFD. Although few errors occur, the tendency is right.

2.2.2 Nonlinear characteristics capture

Fig 1~Fig 3 has shown the good performance for large α prediction. Fig 4 and Fig 5 are the prediction curves at different *Re* and different *Ma* respectively.

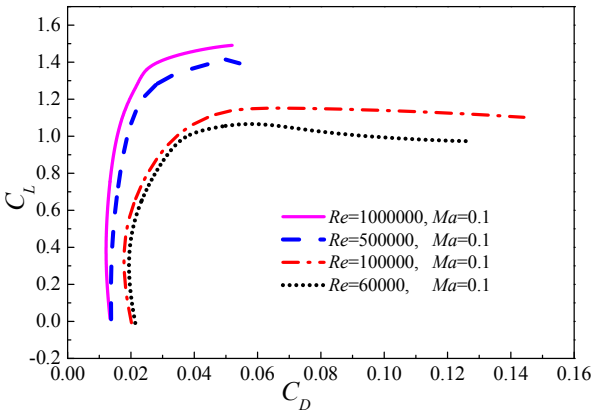

Fig 4 C_L-C_D Prediction of ANN at different *Re*

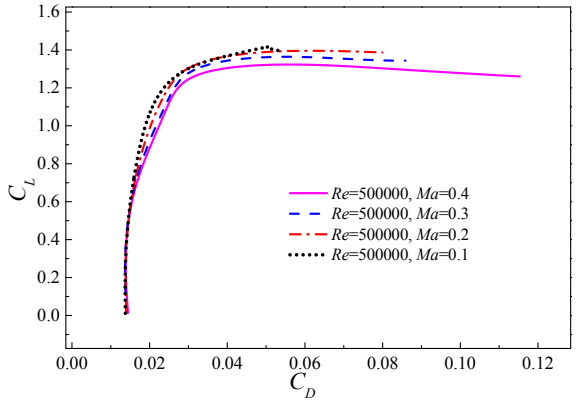

Fig 5 C_L-C_D Prediction of ANN at different *Ma*

Shown as Fig 4, when *Re* decreases, zero lift drag will increase, while maximum lift coefficient, lift-drag ratio and lift line slop will decrease. This result consistent with researches of Silverstein[2].

Shown as Fig 5, when *Ma* increases, zero lift drag will increase, while maximum lift coefficient and lift-drag ratio will decrease. Besides, the effect of *Ma* will increase when α increase.

In general, the ANN airfoil prediction model can reflect the multi-nonlinear effect of the blade element.

3 Limitation and improvement of BEMT

3.1 Limitation of basic BEMT

Veldhuis L L M[3] and LIU Peiqing[4] has discussed the Basic BEMT in detail. The forces and velocity components of a blade element are shown as Fig 6.

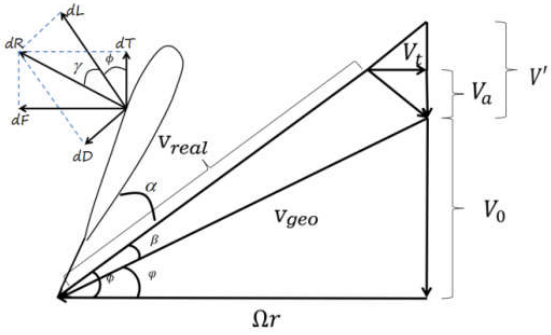

Fig 6 Blade element forces and velocity components

In Fig 6, V_0 is income velocity; β is induced angle; V_t is tangential induced velocity; V_a is axial induced velocity; Ω is rotational velocity (*rad*/*min*). The key step of BEMT is to solve the induced angle in the implicit equation by iteration:

$$C_L\sigma = \frac{4\sin(\varphi+\beta)\tan\beta}{1-\tan\gamma\tan\beta} \quad (1)$$

Where

$$\sigma = \frac{N_B b}{2\pi r} \quad (2)$$

$$\gamma = \arctan\frac{dD}{dL} \quad (3)$$

$$\varphi = \arctan\frac{V_0}{2\pi r n_s} \quad (4)$$

In the equation, φ is geometry angle of attack; σ is blade solidity; γ is angle of lift; N_B is number of blade; b is chord of blade element; r is local radius of the blade element; n_s is rotational velocity (rotations/*min*).

At the condition in which nonlinear effect is not significant and advance ratio is moderate, the equation can be solved and therefore obtain the accurate prediction for thrust and power. However, when the nonlinear effect is considered, such as the large angle of attack condition effect which is included in ANN, or the advance ratio is high, the equation sometimes is difficult to solve. As an example, sometimes the equation will derive the wrong β and obtain the circulation distribution shown as Fig 7~Fig 8.

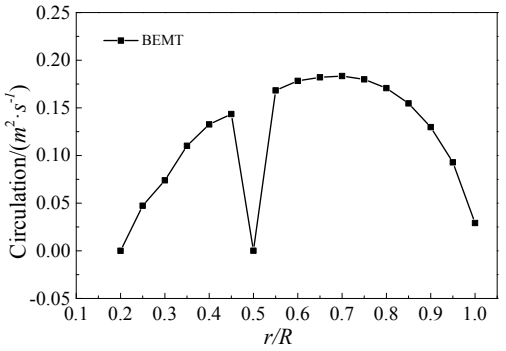

Fig 7 Bad solution at high advance ratio

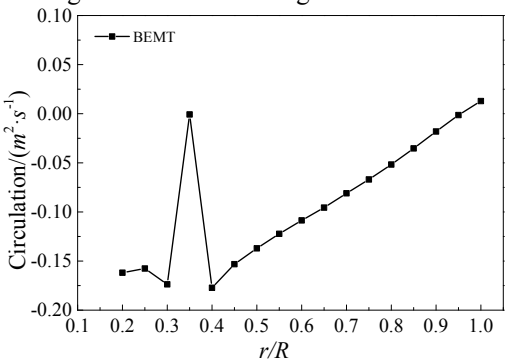

Fig 8 Bad solution at low advance ratio

As Fig 7 and Fig 8 showing, the circulation jump to zero at some radius location. The zero-jumping is caused by wrong solution of the β equation. Consider the condition when the C_L tend to zero ($C_L \to 0$), the denominator on the right hand side of the equation (1) tend to infinite ($1-\tan\gamma\tan\beta \to \infty$). Therefore, $C_L==0$ is always the solution of the equation. This conclusion reveals the non-uniqueness of the equation solution.

The non-uniqueness of the solution reduces the robustness and reliability of BEMT, especially facing the extreme condition, such as extremely low or high advance ratio[8]:

1) At extremely low advance ratio, such as zero free-stream velocity condition, the blade element working at high angle of attack, the nonlinearity of C_L is significant. But when solving the equation, C_L is set as a constant. Therefore, the equation is more likely to obtain non-physical solution.

2) At extremely high advance ratio, the blade element working at small lift condition ($C_L \to 0$), therefore the real solution and non-physical solution are close to each other, resulting to the non-physical solution sometimes.

VTOL-UAV propeller design should consider both zero free-stream condition and high speed condition, but basic BEMT is limited by its non-uniqueness solution.

3.2 Improvement of BEMT

To deal with the singularity problem and the bad solution, an iteration of circulation using both vortex theory and BEMT is shown as Fig 9.

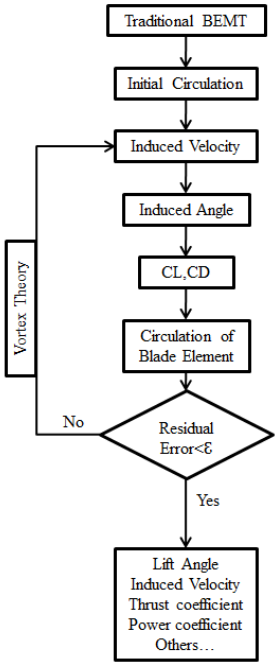

Fig 9 BEMT improvement by Vortex Theory

First, calculate the circulation using BEMT and regard it as initial circulation. Second, calculate induced velocities using vortex theory and then the induced angle and C_L. Third, calculate new circulation with new C_L. With the new circulation next loop can be repeated, until the residual error is lower than given value.

In vortex theory, induced velocity can be written as follows[5].

Axial induced velocity:

$$V_a = \frac{N_B \Omega \Gamma(r)}{4\pi(V_0 + V')} \tag{5}$$

Tangential induced velocity:

$$V_t = \frac{N_B \Gamma(r)}{4\pi r} \tag{6}$$

Where the Γ is circulation, V' is the induced increment of slipstream spiral pitch. In vortex theory, V' is set to be a constant (Betz's condition[6]), but it will change in many conditions.

In order to calculate V', consider the geometric relation of velocity components and obtain:

$$\tan\phi = \frac{V_a + V_0}{\Omega r - V_t} \tag{7}$$

$$V' - V_a = V_t \tan\phi \tag{8}$$

Therefore,

$$V' = \frac{\frac{N_B \Omega \Gamma}{4\pi(V_0 + V')} + V_0}{4\pi\Omega r^2 - N_B\Gamma} N_B\Gamma + \frac{N_B\Omega\Gamma}{4\pi(V_0 + V')} \tag{9}$$

Simplify the equation and write it as a function of Γ:

$$\Gamma(r) = \frac{4\pi(V_0 + V')V'\Omega r^2}{N_B[(V_0 + V')^2 + \Omega^2 r^2]} \tag{10}$$

If circulation distribution is known, the above equation can be solved and obtain V'. In fact, the function(10) is Betz's best circulation distribution at given constant V'.

In reference [7], with the assumption that induced velocity (V_t+V_a) is perpendicular to real inflow velocity (V_{real}), the relation of V_t and V_a can be written as follows:

$$V_a = \frac{V_t}{\tan\phi} \tag{11}$$

Solving V' cost much time than above formula, so if φ is obtained one can use above formula to calculate V_a.

Once V_t and V_a are obtained, induced angle β can be calculate from geometry relation, which avoids the non-physical solution of β equation. The iteration can correct the bad solution from basic BEMT.

3.3 Result of refined BEMT

With the circulation-iteration correction introduced above, two typical examples are shown in this section. In these examples, JXF16×8 propeller is used, whose diameter is 16in, and the blade was separated to 17 sections from 0.2R to R. In the following figures, the circulation results from BEMT and refined BEMT (rBEMT) are compared.

3.3.1 Extremely low advance ratio

Considering the working condition as follows: V_0=0.1m/s, n=948.65r/min, J=0.016, H=400m, the circulation comparisons between refined and basic BEMT are shown as following figure.

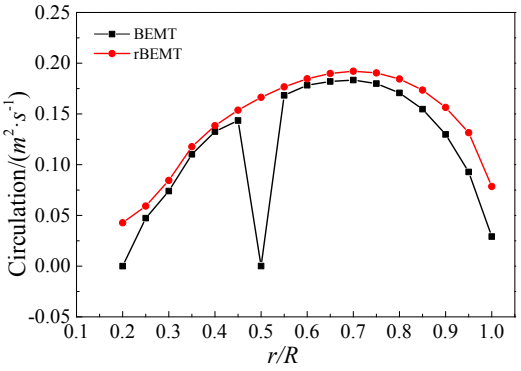

Fig 10 Circulation at low advance ratio

At this condition, blade elements have large nonlinear effect. Basic BEMT obtains a wrong solution at 0.5R, which result from the non-uniqueness of the equation solution. However, the blade element at 0.5R which working at positive angle of attack must generates positive C_L. By comparison, the refined BEMT corrected the wrong solution using circulation iteration.

3.3.2 Extremely high advance ratio

Considering the working condition as follows: V_0=40km/h, n=2200r/min, J=0.7456, H=400m, the circulation comparisons are shown as following figure.

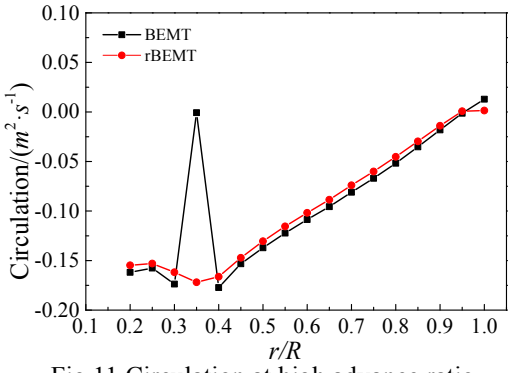

Fig 11 Circulation at high advance ratio

At this condition, blade elements work at low-lift condition. Therefore, the solutions are closed to non-physical solution (C_L==0). For this reason, basic BEMT obtains a non-physical solution at 0.35R. However, the circulation shows a normal distribution after circulation-iteration correction.

4. Verification

In order to show that this method has good accuracy and robustness at both normal and extreme conditions, this section shows the

comparison between rBEMT and CFD or propeller test.

4.1 Propeller vehicle test

Fig 12 is a schematic diagram of a propeller vehicle test system. A six component balance was used to measure the pulling force and torque of the propeller. The data collector is directly connected with the six component balance and the computer. The motor is fixed on the six component balance, and the balance is fixed on the pole that is extended by the carriage. The flow velocity range is about 0-50km/h, the power range is about 0-300W, and the altitude is 450m. Fig 13 and Fig 14 are photos of balance, data collector and vehicle test.

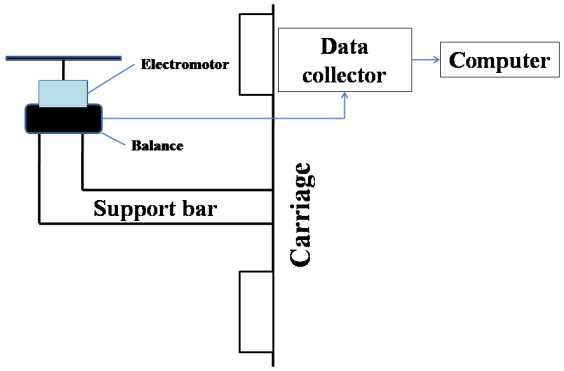

Fig 12 Testing system

Fig 13 Six-component balance (left) and data collector (right)

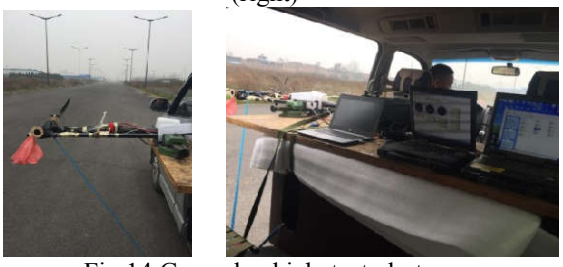

Fig 14 Ground vehicle test photos

The discrete points obtained by the experiment are fitted as a curve of advance ratio, which can be converted into curves of rotation speed at given inflow velocity. However, the tested data at zero inflow velocity are used directly because it cannot be obtained from the curve of advance ratio. Fig 15 and Fig 16 are examples of test data.

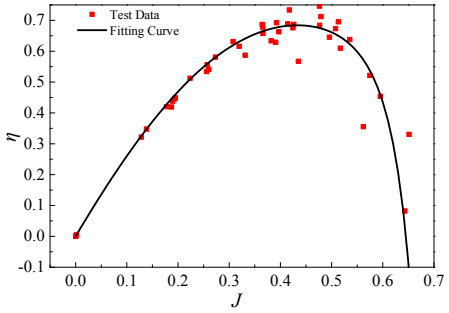

Fig 15 Examples of test data (efficiency)

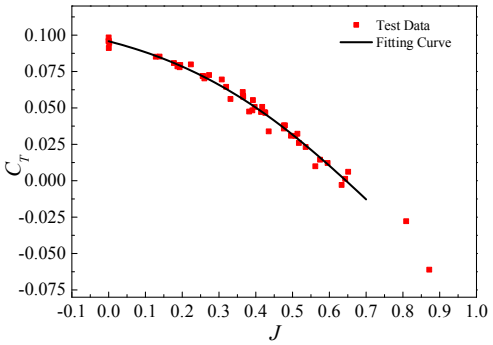

Fig 16 Examples of test data (C_T)

Other curves are shown in following part in comparison with rBEMT.

4.2 Result and discussion

In comparison, the propeller was also analyzed by CFD. In this paper, turbulence model is k-ω SST, while the mesh type is structured-unstructured hybrid grid, and multiple reference frames (MRF) is used for simulation of propeller rotation. The size of unstructured meshes in the rotating domain is 955.981 thousand, while the size of structured meshes in static domain is 2811.478 thousand. Calculation condition: inflow velocity V_0=0.4063m/s (preset velocity for convergence at static state), altitude H=400m, and rotation speed of propeller n=1000~5000r/min.

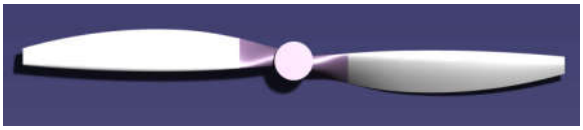

Fig 17 Geometry of JXF 16×8 propeller

The dark part of the Fig 17 is regarded as the hub of the propeller (r<0.2R), which is not included in BEMT but is included in CFD model. The blade is divided into 17 parts in BEMT.

The results of rBEMT and CFD in comparison with test data are shown as follows.

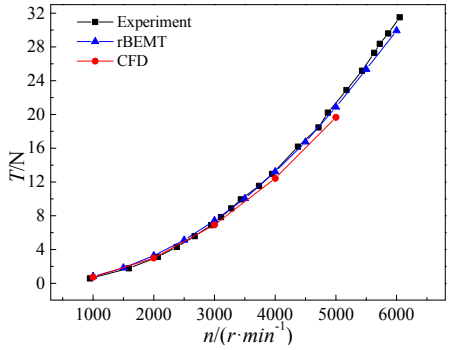

Fig 18 JXF 16×8 Propeller at 0*km/h* (Thrust)

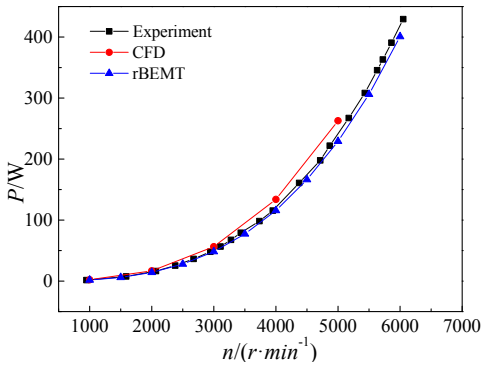

Fig 19 JXF 16×8 Propeller at 0*km/h* (Power)

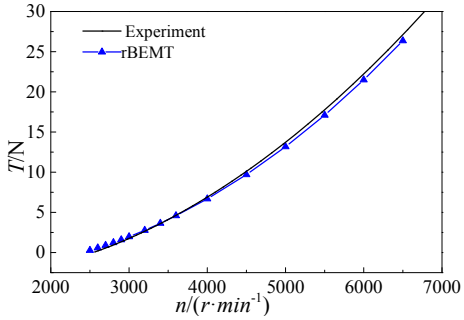

Fig 20 JXF 16×8 Propeller at 40*km/h* (Thrust)

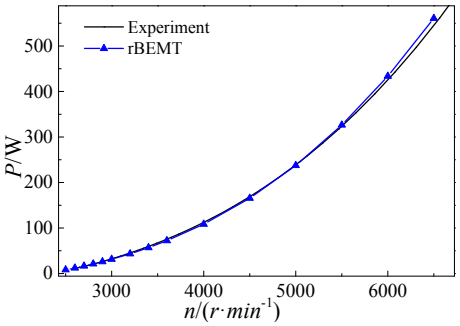

Fig 21 JXF 16×8 Propeller at 40*km/h* (Power)

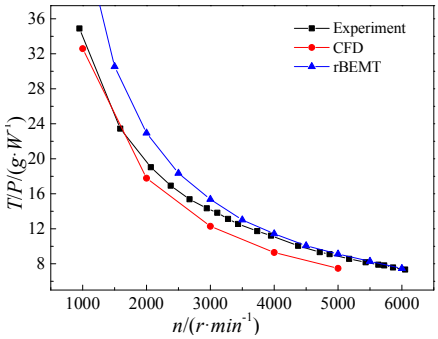

Fig 22 *T*/*P* at static condition (*g*/*W*)

As shown above, thrust and power results of rBEMT are in good agreement with the CFD and experimental results. The relative error of thrust and power is less than 5%. The reasons for the error may be the following.

1) Geometric modeling error. The tip geometry is slightly different between CAD model and physical model.

2) In rBEMT, the influence of hub is ignored. However, the influence of hub, such as drag, will become significant in the case of low thrust. Therefore, *T*/*P* is higher than test data at low thrust condition.

3) A bracing rod is connected to the rear of the hub in experiment, while the downstream of the propeller in CFD is empty. Therefore, the pressure drag of hub reduces the thrust of propeller.

In order to verify the robustness and reliability of rBEMT in different altitude, several condition is analyzed: *H*=500*m* (12*m*/*s*), 3000*m* (15*m*/*s*), 10000*m* (20*m*/*s* & 33*m*/*s*). The comparison between rBEMT and CFD results are shown as follows.

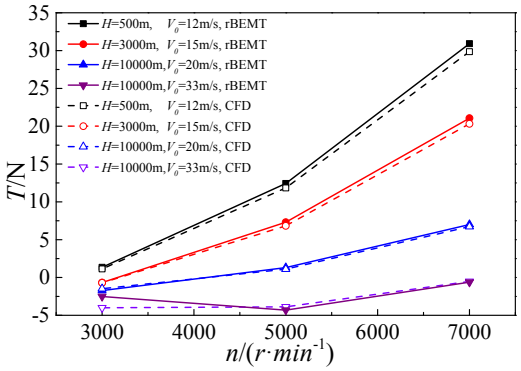

Fig 23 Thrust of JXF16×8 propeller at different height

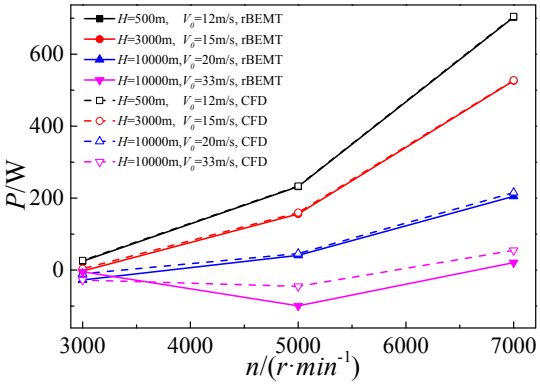

Fig 24 Power of JXF16×8 propeller at different height

In Fig 23 and Fig 24, the comparison shows good agreement of rBEMT and CFD, where the relative error is generally lower than 5%, except the condition of *H*=10000*m* and

V_0=33m/s. At this condition, the blades are suffering deep stall of negative angle of attack, where the blade element data are obtained from extrapolation and therefore not accurate.

5 Inverse BEMT for propeller design

5.1 Best circulation distribution

5.1.1 Design criteria

Imagine that the circulation at radial position r obtains an increment $\Delta\Gamma$, therefore the thrust and torque increments are ΔT and ΔM respectively, while the useful work and total work increments are $V_0\Delta T$ and $2\pi n_s\Delta M$ respectively. Define an energy ratio k to describe the ratio of useful and total work:

$$k=\frac{V_0\Delta T}{2\pi n_s\Delta M} \tag{12}$$

To obtain the best circulation, circulation should be increased where k is large, but be decreased where k is small. Therefore, the criterion of best circulation distribution is that k should be a constant alone the radial direction.

5.1.2 Best circulation in zero-drag condition

Ignoring the airfoil drag, the increments induced by $\Delta\Gamma$ is:

$$\Delta T=\rho\Delta\Gamma(2\pi n_s r-V_t)dr=\rho\Delta\Gamma(\Omega r-V_t)dr \tag{13}$$

$$\Delta M=\rho\Delta\Gamma(V_0+V_a)rdr \tag{14}$$

Therefore the energy ratio k:

$$k=\frac{V_0\Delta T}{2\pi n_s\Delta M}=\frac{V_0(\Omega r-V_t)}{2\pi n_s(V_0+V_a)} \tag{15}$$

$$\frac{V_0+V_a}{\Omega r-V_t}=\frac{V_0}{2\pi n_s rk} \tag{16}$$

From the geometry relation in Fig 6,

$$\tan\varphi=\frac{V'+V_0}{\Omega r}=\frac{V_a+V_0}{\Omega r-V_t} \tag{17}$$

$$\frac{V'+V_0}{\Omega r}=\frac{V_0}{2\pi n_s rk} \tag{18}$$

To keep k as a constant, the V' should be a constant. In this condition, as derived in section 3.2, the circulation distribution can be written as function(10).

5.1.3 Best circulation in normal condition

The drag of airfoil will lead to the increase of ΔM and the decrease of ΔT.

$$\Delta T=[\rho\Delta\Gamma(\Omega r-V_t)-\Delta D\sin\varphi]dr \tag{19}$$

$$\Delta M=[\rho\Delta\Gamma(V_0+V_a)+\Delta D\cos\varphi]rdr \tag{20}$$

Referring to the definition of circulation, define a "drag circulation" $\Delta\Gamma_D$, which is parallel to the flow direction, such as:

$$dL=\frac{1}{2}\rho V_{local}{}^2C_L bdr=\rho\vec{V}\times\vec{\Gamma}dr \tag{21}$$

$$dD=\frac{1}{2}\rho V_{local}{}^2C_D bdr=\rho\vec{V}\bullet\vec{\Gamma}_D dr \tag{22}$$

$$\Gamma_D(r)=\frac{1}{2}V_{local}C_D(r)b(r)=\Gamma/\frac{C_L}{C_D}(r) \tag{23}$$

Therefore

$$\Delta T=\rho(\Delta\Gamma V_t-\Delta\Gamma_D V_a)dr \tag{24}$$

$$\Delta M=\rho(\Delta\Gamma V_a+\Delta\Gamma_D V_t)rdr \tag{25}$$

For given airfoil and its design angle, the expression of k can be written as

$$k=\frac{V_0}{\Omega r}\frac{\frac{C_L}{C_D}(\Omega r-V_t)-(V_0+V_a)}{\frac{C_L}{C_D}(V_0+V_a)+(\Omega r-V_t)} \tag{26}$$

Take the formula of V_a and V_t into the above formula and obtain

$$\Gamma(r)=\frac{4\pi r}{N_B}\bullet\frac{C_1}{C_2} \tag{27}$$

where

$$C_1=\frac{C_L}{C_D}V_0\Omega r(1-k)-k\Omega^2r^2-V_0^2 \tag{28}$$

$$C_2=\frac{\frac{C_L}{C_D}k\Omega r+V_0}{(V_0+V')}\Omega r+(\frac{C_L}{C_D}V_0-k\Omega r) \tag{29}$$

For given C_L/C_D and k, the circulation distribution can be calculated.

On the other hand, the Prandtl correction[4] is used to consider the effect of number of blade.

As an example, the circulation at Betz condition and normal condition are shown as following figure.

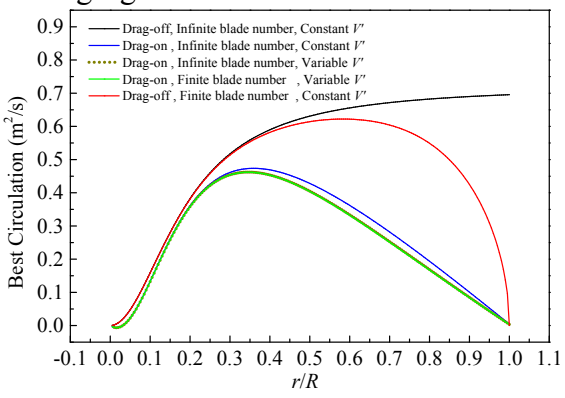

Fig 25 Best Circulation Distribution

To obtain given thrust or power, the k (for normal condition) or V' (for Betz condition) should be change to the appropriate value.

5.2 Inverse BEMT design method

For propeller quick design, an inverse BEMT could be derived. In this way, chord length and twist angle can be calculated at given circulation and C_L distribution.

From the implicit equation(1) of β, the chord length b can be written as a function of C_L, γ and β.

$$b=\frac{2\pi r}{N_B C_L}\frac{4\sin(\varphi+\beta)\tan\beta}{1-\tan\gamma\tan\beta} \tag{30}$$

Meanwhile, the circulation can be written as:

$$\Gamma(r)=\frac{1}{2}V_{local}C_L(r)b(r) \tag{31}$$

where

$$V_{local}=\sqrt{[V_0(a+1)]^2+[2\pi n_s r(a'+1)]^2} \tag{32}$$

a and a' is axial and tangential induction factor namely, which are both function of β and γ [4]. Therefore, the circulation is a function of C_L, C_D and β.

$$\Gamma(r)=f_\Gamma(C_L,C_D,\beta) \tag{33}$$

If the airfoil data at design angle of attack is obtained at the beginning of the design process, C_L and C_D are known. Once the circulation distribution is given, the equation is closed and β can be calculated by numerical method. Then, the chord length b can be calculated and twist angle can be obtained.

Using this method, one can obtain chord and twist angle quickly at given design angle and circulation distribution. If the chord distribution is given, the design angle of attack should be changed in radial direction. By the iteration method, the design angle of attack and twist angle can also be obtained at given chord distribution and circulation, except when the chord length is too small to obtain reasonable C_L. Once the design angle of attack is determined, one can choose or design better airfoil in different radial positions.

5.3 Propeller design examples

To show the design accuracy of inverse BEMT, a design example was presented. The propeller diameter is 0.4064m, income flow velocity is 13m/s, rotation speed is 4000r/min, with two blades. The given target circulation and design result is shown as following figure, where the airfoil drag is considered in the best circulation.

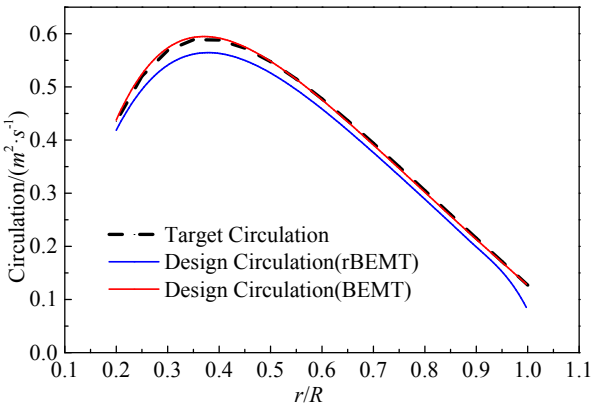

Fig 26 Target and designed circulation

The design-circulation from inverse BEMT is consistent with the target-circulation. After the refinement of circulation-iteration, the value of circulation decreased slightly. However, the inverse design method will offer accurate result for given circulation. The chord length and twist angle are shown as Fig 27. As comparison, another propeller designed with zero-drag circulation is also shown.

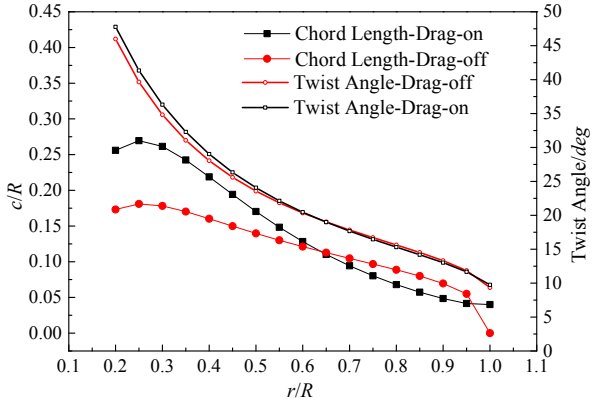

Fig 27 Chord and incident angle distribution

And the performance of the design result is shown as follows:

Table 2 Propeller performance at designed condition

method(drag)	T/N	M/($N\cdot m$)	P/W	η
BEMT(On)	5.2149	0.20888	87.4966	77.482%
rBEMT(On)	5.0469	0.20661	86.5426	75.813%
rBEMT(Off)	5.0321	0.20610	86.3320	75.774%

The performance of design result is close to the performance of JXF 16×8 propeller. The

quick design by inverse BEMT can obtain a result that can be used as initial model of optimization.

It can be seen that the common propeller shape is designed by the Betz condition. The best circulation which considers the airfoil drag leads to a different chord length distribution. However, the difference of efficiency is not huge.

Notice that the C_L/C_D was assumed to be a constant alone the radial direction, the design result by above method may improve by optimization.

6. Conclusion

1) The BP neural network is applied to establish the nonlinear aerodynamic analysis model of airfoil, which can provide efficient nonlinear aerodynamic prediction for blade element in BEMT.

2) Equation of induced angle in basic BEMT has non-physical solution, which results in the decrease of calculation robustness, especially at low/high advance ratio. In this paper, circulation iteration is applied to improve the robustness and reliability of BEMT.

3) The analysis examples show that the modified BEMT results are accurate, the relative error of force and power are less than 5% at normal condition, while the relative error are less than 10% at extreme low/high advance ratio condition.

4) The design method derived from inversed BEMT can be used to design high efficiency propeller with given circulation distribution. The best circulation which considers the airfoil drag leads to a different chord length distribution from Betz condition.

Reference

[1] Haykin Simon. *Neural Networks and Learning Machine*. Beijing, Machinery Industry Press, 2011.

[2] Silverstein Abe. Scale effect on Clark Y airfoil characteristics from NACA full-scale wind-tunnel tests. *Technical Report Archive & Image Library*. 1935.

[3] Veldhuis L L M. Propeller Wing Aerodynamic Interference. *Aerospace Engineering*, 2005.

[4] LIU Peiqing. *Theory and application of airscrew*. Beihang University Press, 2006.

[5] CAO Yihua. *Aerodynamics of Modern Helicopter Rotors*. Beihang University Press, 2015.

[6] Adkins C N, Liebeck R H. Design of optimum propellers. *Journal of Propulsion & Power*, 1994, 10(5):676-682.

[7] T. Theodorsen. *Theory of Propellers*. New York, McGraw Hill, 1948.

[8] Nigam, Nikhil, et al. Multi-Fidelity Multi-Disciplinary Propeller/Rotor Analysis and Design. *Aiaa Aerospace Sciences Meeting*, 2013.

[9] Morgado J, Silvestre M A R, Pascoa J C. Full range airfoil polars for propeller blade element momentum analysis. *American Institute of Aeronautics and Astronautics Inc*., 2013.

[10] Dorfling J, Rokhsaz K. Non-linear aerodynamic modeling of airfoils for accurate blade element propeller performance predictions. *American Institute of Aeronautics and Astronautics Inc*., 2014.

[11] Macneill R, Verstraete D. Blade element momentum theory extended to model low Reynolds number propeller performance. *Aeronautical Journal*. 2017, 121(1240): 835-857.

[12] Martínez J, Bernabini L, Probst O, et al. An improved BEM model for the power curve prediction of stall-regulated wind turbines. *Wind Energy*. 2005, 8(4): 385-402.

[13] Dossing M. A detailed investigation of the corrected BEM method and the potential for improving blade design. *European Wind Energy Association*, 2009.

[14] Whitmore S A, Merrill R S. Nonlinear large angle solutions of the blade element momentum theory propeller equations. *Journal of Aircraft*. 2012, 49(4): 1126-1134.

[15] Barnes J P. Hybrid lifting-line/blade-element method for propeller or propfan performance. *American Institute of Aeronautics and Astronautics Inc*, AIAA, 2017.

Contact Author Email Address

yingfengFZY@163.com

Copyright Statement